Supplementary Figure Legends

Supplementary Figure 1. Differential expression of CIRBP isoforms in clinical samples and breast cancer cells.

(a) CIRBP-S mRNA expression in non-metastatic versus metastatic breast cancer samples (left) and in non-TNBC versus TNBC tumors (right) in public cohorts. (b) The expression of CIRBP-S protein in breast cancer cell lines with low metastatic potential (T47D, MCF7 and BT474) or high metastatic potential (MDA-MB-157, MDA-MB-231 and Hs578T) was analyzed with western blotting. GAPDH was used as loading control for western blotting.

Supplementary Figure 2. CIRBP-L functioned as a metastasis suppressor in breast cancer cells.

(a) Validation of CIRBP-L knockdown in MCF7 cells (shScramble *vs* shCIRBP-L) and CIRBP-L overexpression in MDA-MB-231 cells (Control *vs* CIRBP-L OE) by RT–qPCR and immunoblotting. Cyclophilin and GAPDH was used as the normalization control, respectively. (b) CIRBP-S expression in CIRBP-L–modulated cells measured by RT–qPCR and immunoblotting, showing CIRBP-L manipulation did not alter CIRBP-S levels. (c) Quantification of human vimentin IHC staining scores of lung sections from the experimental metastasis model (related with Fig. 2d). Results are presented as means ± SDs. **P < 0.01; ns, not significant (two-tailed Student's t-test).

Supplementary Figure 3. CIRBP-L enhanced microtubule acetylation and polymerization through HDAC6 regulation.

(a) Quantification of relative microtubule polymerization in CIRBP-L–modulated breast cancer cells, as determined using band intensities of soluble (S) and pellet (P) fractions and expressed relative to unmodified control cells (related with Fig. 3b). (b) Immunoblot analyses of acetylated α-tubulin after SIRT2 (AGK2, 10 μM) or HDAC1 (Entinostat, 10 μM) inhibition in the indicated CIRBP-L knockdown cells. GAPHD was used as loading control. Results are presented as means ± SDs. *P < 0.05 (two-tailed Student's t-test.

Supplementary Figure 4. CIRBP-L increased DCLK1-L protein through translational regulation.

(a) HDAC6 mRNA and protein levels in CIRBP-L–modulated MCF7 and MDA-MB-231 cells as determined by RT–qPCR and western blotting. (b) Immunoblot analysis of DCLK1-L protein levels across breast cancer cell lines with low or high metastatic potential. (c) DCLK1-L mRNA levels across the same panel of cell lines as determined by RT–qPCR. (d) DCLK1-L mRNA levels in CIRBP-L–modulated MCF7 and MDA-MB-231 cells. (e) DCLK1-L mRNA stability assessed by actinomycin D chase and subsequent RT–qPCR in CIRBP-L–modulated cells; remaining DCLK1-L mRNA (%) is with respect to time 0. Cyclophilin and GAPDH were used as normalization controls for RT-qPCR and western blotting, respectively. (f) Schematic of DCLK1-L mRNA fragments and luciferase reporter constructs used to assess CDS-dependent translational regulation.

Supplementary Figure 5. DCLK1-L was essential for the CIRBP-L–mediated inhibition of breast cancer metastasis.

(a) Wound-healing migration assays in CIRBP-L knockdown MCF7 cells with or without

DCLK1-L restoration, and in CIRBP-L–overexpressing MDA-MB-231 cells with or without DCLK1 knockdown, as indicated. Quantitative analysis was performed using ImageJ software (related with Fig. 5a). (b) Transwell invasion assays in the same experimental settings. Invaded cells were quantified with ImageJ software (related with Fig. 5b). (c) Quantification of human vimentin IHC staining in lungs from the experimental colonization model (related with Fig. 5c), shown as vimentin IHC scores. Results are presented as means ± SDs. *P < 0.05, **P < 0.01 (two-tailed Student's t-test).

Supplementary Figure 6. DCLK1-L suppressed HDAC6 activity via GSK3β Ser9 phosphorylation.

(a) Co-immunoprecipitation assays were used to assess the association between Myc–DCLK1-L and Flag–HDAC6 in HEK293 cells. Input controls confirmed the expression of transfected constructs. (b) Immunoblotting was used to assess the effect of GSK3β inhibition (LiCl) on α-tubulin polymerization in cells modulated with CIRBP-L or DCLK1-L. GAPDH was used as the loading control.

Supplementary Table S1. List of RT-qPCR primer sequences used in this study

Gene	Forward (5′ to 3′)	Reverse (5′ to 3′)
CIRBP-L	ACCTTGCTCTGACAATTCCCT	TGGGCCTCCCTTTCTAGCTC
CIRBP-S	CAGTTACGCTACACACAACG	ACGTTCAGCGAAGCTCCCAC
DCLK1-L	GGTGAACGTCAAGACCACCT	GAGCCGTTTTCTTGTTCAGC
HDAC6	ACTGCAAGGGATGGATCTGA	GTTGCTCCTTGATGGCATGG
Cyclophilin	TGCCATCGCCAAGGAGTAG	TGCACAGACGGTCACTCAAA

Supplementary Table S2. The target sequences of shRNA used in this study

Primers	Sequences
CIRBP-L	CCGG GG AAA TAG CCC TGT AAT TAC TCG AGT AAT TAC AGG GCT ATT TCC T TT TTG
DCLK1-L	CCGG AC CCG AAC TCT GTC GGA TAA CCT CGA GGT TAT CCG ACA GAG TTC GGG T TT TTT G

Supplementary Table S3. List of primers used for mutagenesis

Primers	Sequences
DCLK1-D511N-F	GAT CAT CGT CCA CCG TAA TAT CAA GCC A
DCLK1-D511N-R	GAT CTG GCT TGA TAT TAC GGT GGA CGA T

Supplementary Figure 1. Differential expression of CIRBP isoforms in clinical samples and breast cancer cells

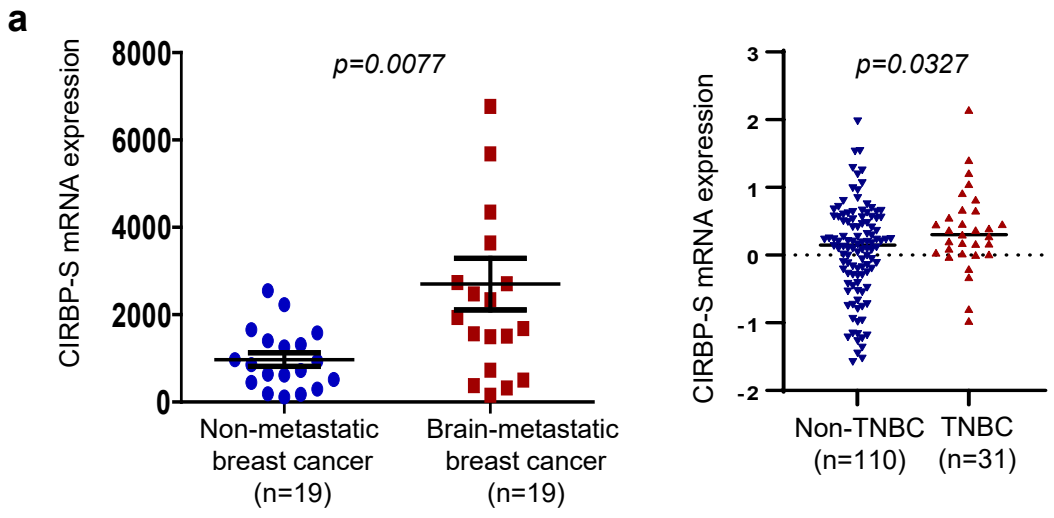

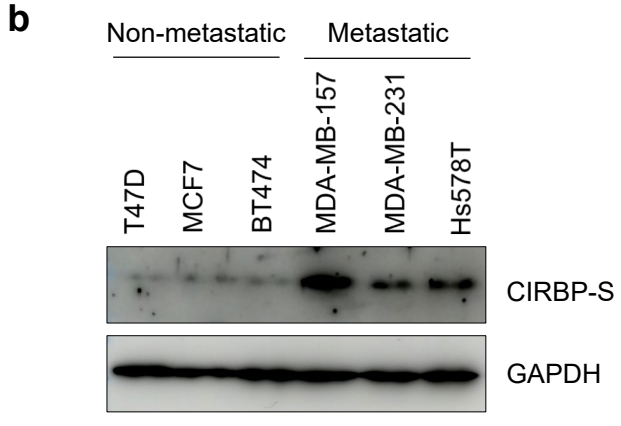

Supplementary Figure 2. CIRBP-L functioned as a metastasis suppressor in breast cancer cells

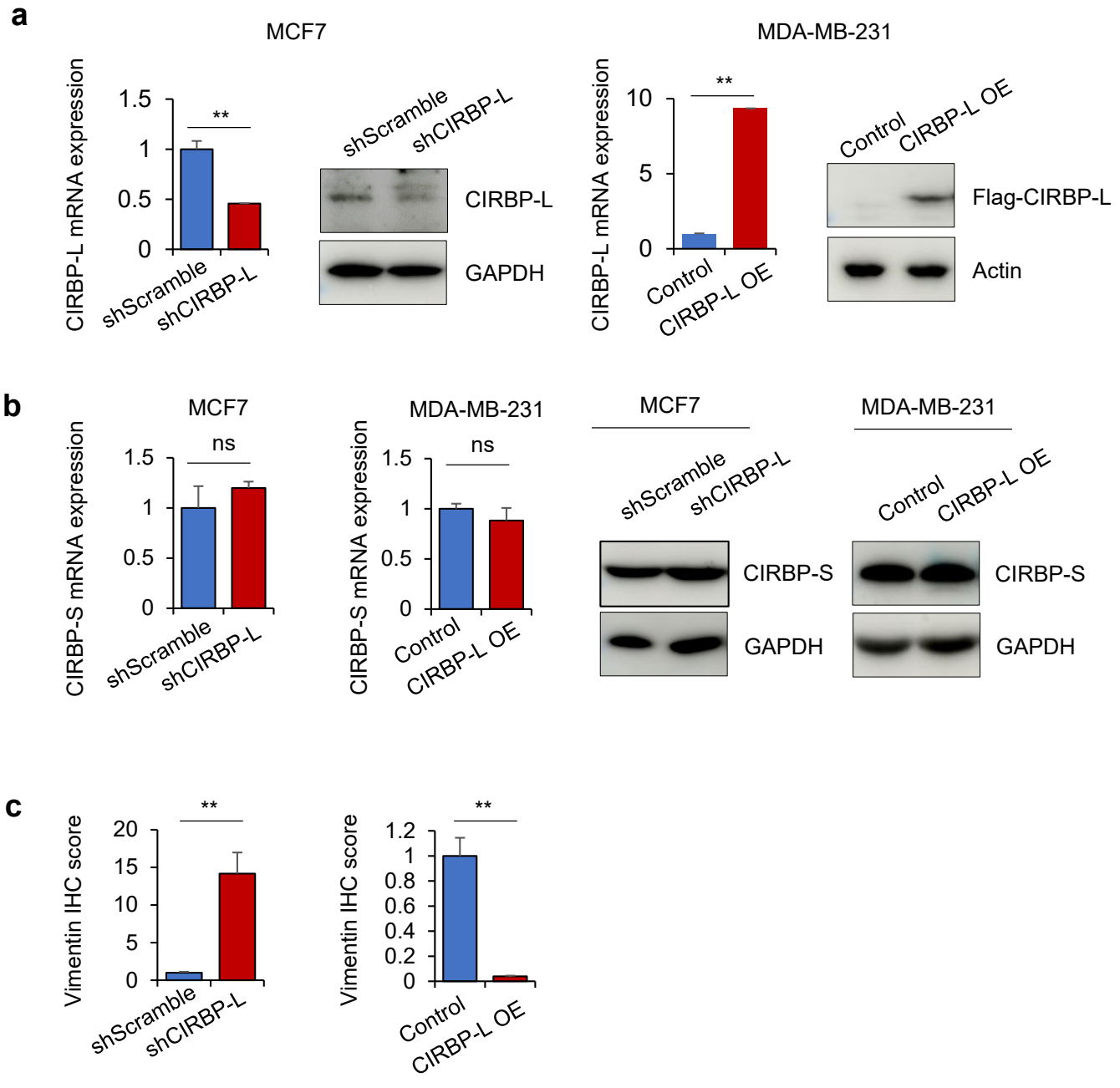

Supplementary Figure 3. CIRBP-L enhanced microtubule acetylation and polymerization through HDAC6 regulation

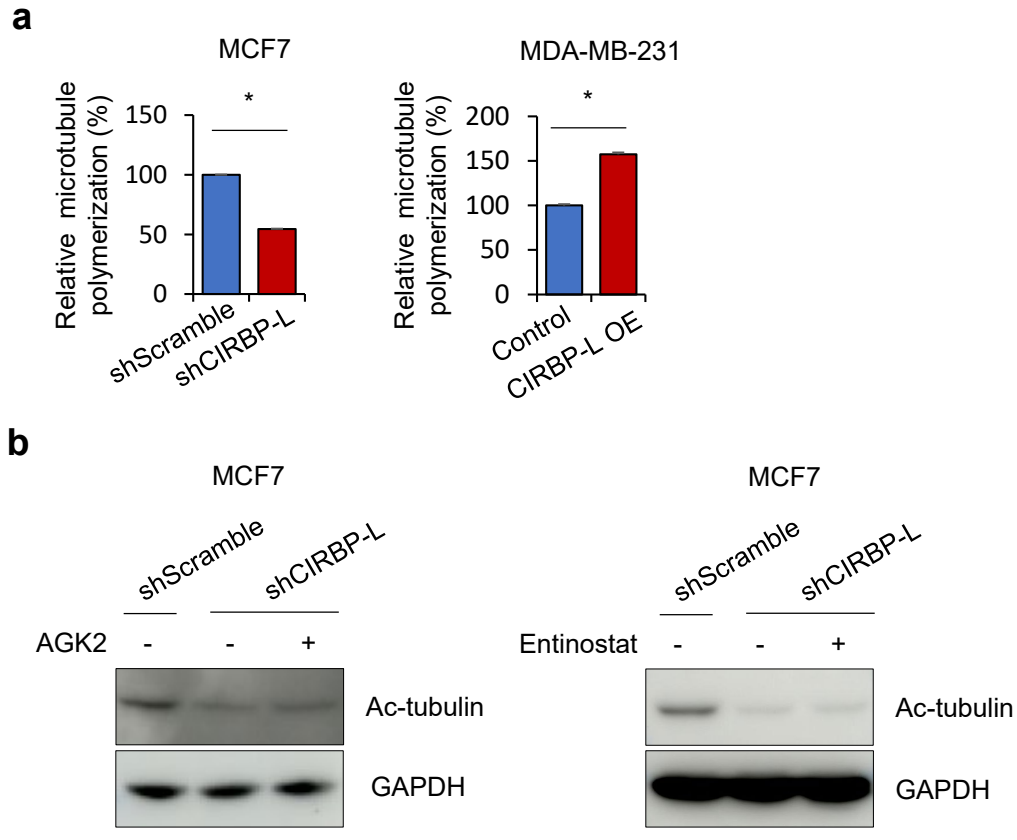

Supplementary Figure 4. CIRBP-L increased DCLK1-L protein through translational regulation

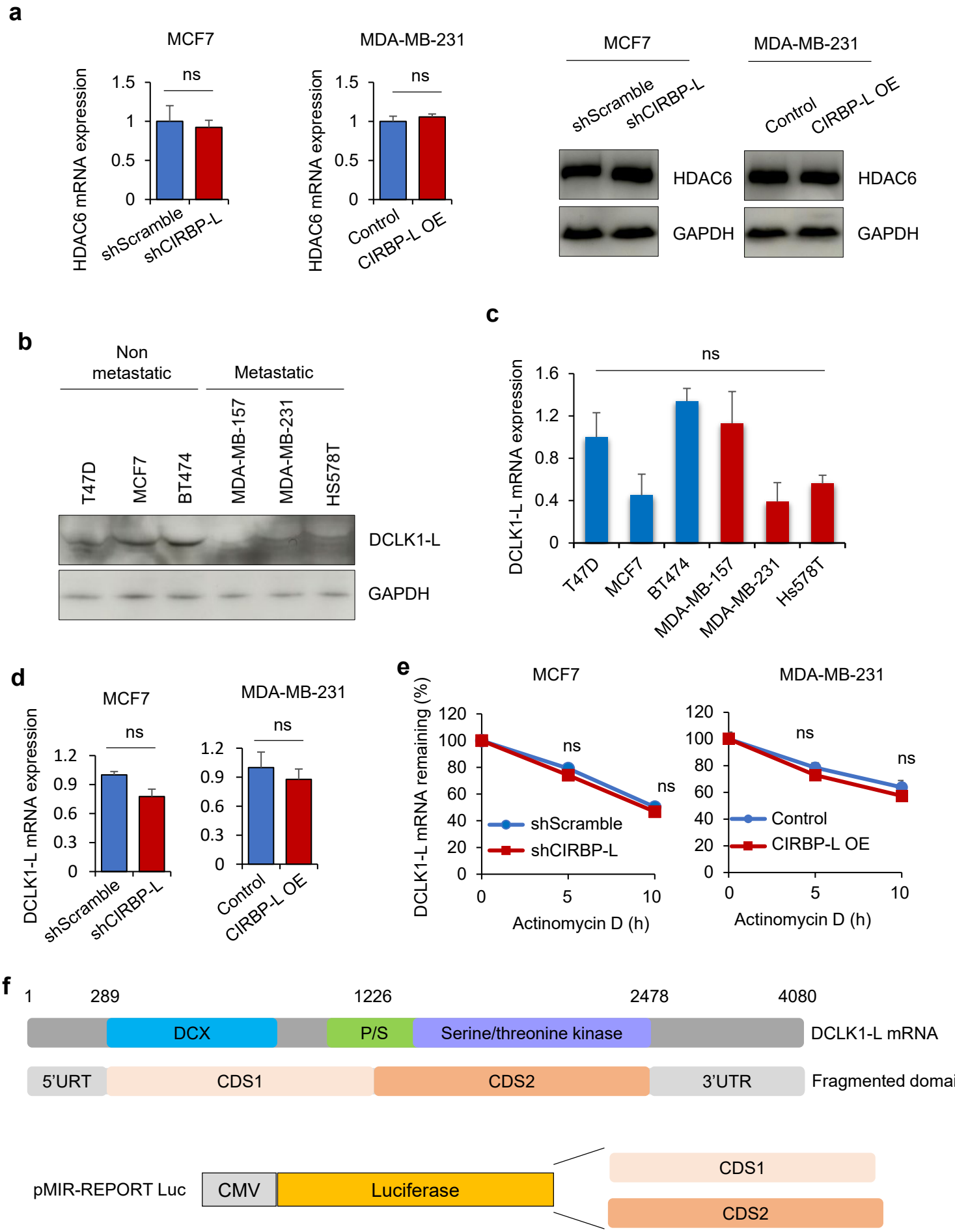

Supplementary Figure 5. DCLK1-L was essential for the CIRBP-L-mediated inhibition of breast cancer metastasis

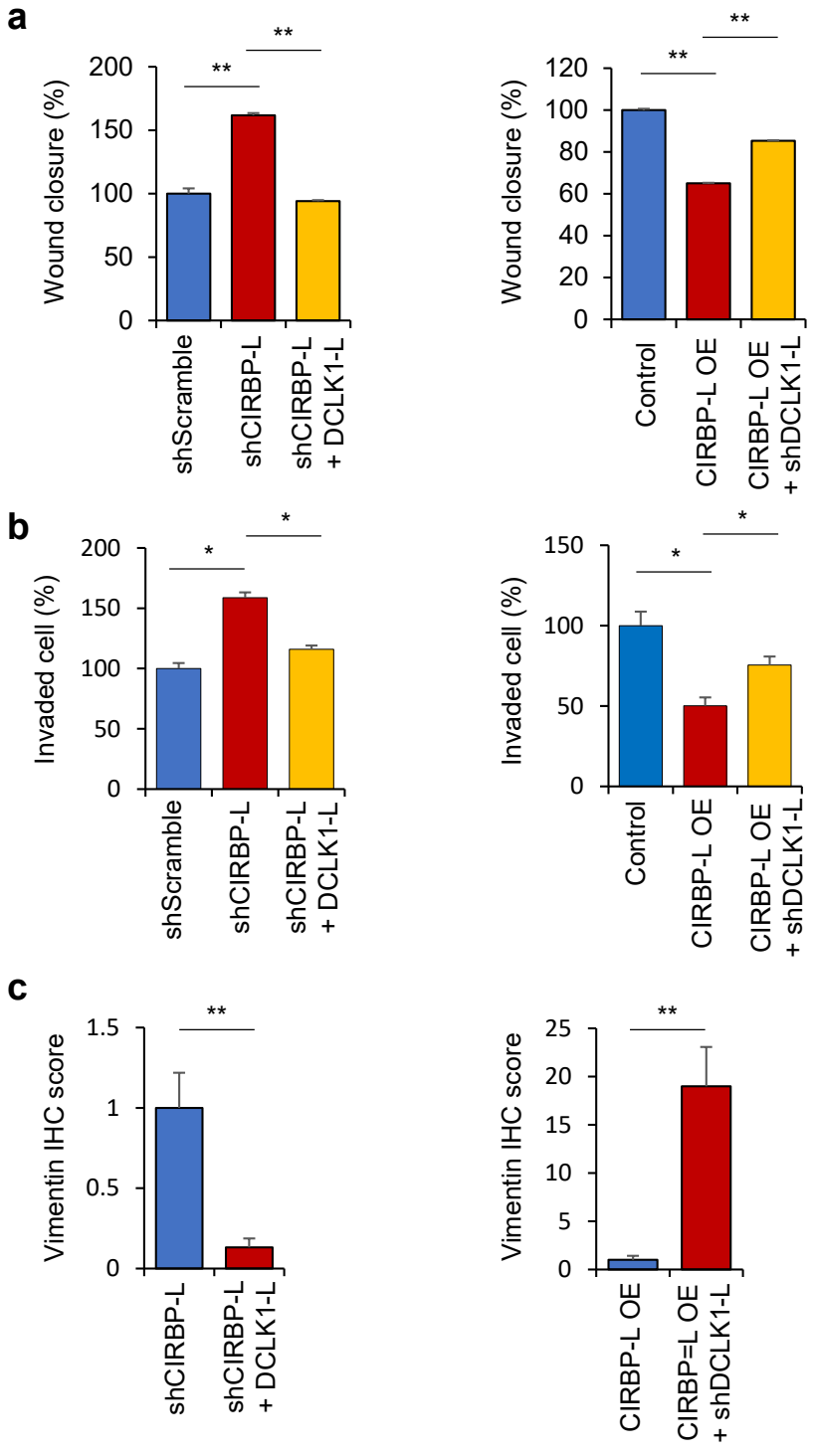

Supplementary Figure 6. DCLK1-L suppressed HDAC6 activity via GSK3β Ser9 phosphorylation